European Polymer Journal 235 (2025) 114084

Contents lists available at ScienceDirect

European Polymer Journal

journal homepage: www.elsevier.com/locate/europolj

On a promising and effective combination of epoxidized soybean oil acrylate with N-isopropylacrylamide in the development of cross-linked materials

Martina Cozzani [a], Daniele Nuvoli [b], Alberto Mariani [a], Orietta Monticelli [a,*]

[a] Dipartimento di Chimica e Chimica Industriale, Università di Genova, Via Dodecaneso 31, 16146 Genova, Italy
[b] Dipartimento di Scienze Chimiche, Fisiche, Matematiche e Naturali, Università di Sassari, and INSTM, Via Vienna 2, 07100 Sassari, Italy

ARTICLE INFO

Keywords:
Epoxidized soybean oil acrylate
Poly(N-isopropylacrylamide)
Frontal polymerization
Mechanical properties
Retention capacity

ABSTRACT

With the aim of expanding the application possibilities of a derivative of soybean oil, namely epoxidized soybean oil acrylate (ESOA), a compound from renewable sources, by giving it functional and structural properties, the development of its formulations was investigated in this work. ESOA was combined with N-isopropylacrylamide (NIPAAm) by a reactive radical process to modify not only the features of the oil but also those of poly(N-isopropylacrylamide) (PNIPAAm), in particular to improve its mechanical properties and its retention capacity for hydrophobic molecules. The formulations, based on different ratios of ESOA/NIPAAm, were prepared using trihexyl tetradecyl phosphonium persulfate (TETDPPS) as a non-gas-releasing radical initiator, and applying a very energy-efficient polymerization method, *i.e.*, frontal polymerization.

The investigation of the polymerization front velocity (V_f) and the front temperature (T_{max}) showed a significant dependence of these two parameters on the ratio of the two components, with an increase in T_{max} and V_f with the amount of NIPAAm and with a limit of front formation up to an ESOA/NIPAAm ratio of 90. As indicated by the microscopic measurements, the prepared formulations showed a decreasing porosity with increasing ESOA amount, while the DSC analyses proved a good compatibility between the components, which was favored by the formation of a copolymeric system during the free radical polymerization process. The mechanical properties were investigated by DMA compression analyses, which revealed a relevant increase in modulus when increasing the ESOA content in the reaction mixture. It was also found that the swelling and the ability to retain hydrophobic compounds depends on the initial composition, with the former parameter decreasing with increasing the ESOA/NIPAAm ratio and the retention capacity increasing significantly with increasing ESOA content in the reaction mixture.

1. Introduction

The development of novel formulations based on compounds from renewable sources is attracting considerable interest, as they address the need to limit the use of materials from fossil sources and, in some cases, these systems are derived from agricultural processing, thus reducing the impact of waste [1,2]. Among the various bio-based materials, those derived from soy, such as soybean oil or modified soybean oil, are particularly promising [3,4]. Indeed, the above-mentioned compounds can be modified in various ways to make them more usable for different applications [5–7]. In particular, Sharma et al. [5] successfully produced acyl derivatives of vegetable oils from epoxidized soybean oil and a series of acid anhydrides in a one-pot synthesis. The resulting derivatives proved to be suitable for the development of industrial lubricant formulations [6]. In a more recent study, Amos et al. [7] carried out the maleation of soybean oil in a pilot plant scale, obtaining a sustainable alternative to alkenyl succinic anhydrides, which are commonly used to modify polysaccharides to enhance their applicability in food additives, binders in papermaking and adhesives. Moreover, various studies dealt with the acrylation of epoxidized soybean oil [8,9], whose acrylic functionalities allow the resulting material to be used in radical reactions and also to be combined with other polymer systems through reactive processes. Mauck et al. [10] took advantage of this feature by using epoxidized soybean oil acrylate (ESOA) as a modifier to improve

* Corresponding author.
E-mail address: orietta.monticelli@unige.it (O. Monticelli).

https://doi.org/10.1016/j.eurpolymj.2025.114084
Received 3 February 2025; Received in revised form 29 May 2025; Accepted 20 June 2025
Available online 20 June 2025

the toughness of polylactic acid (PLA), thus developing a biodegradable and renewable alternative to petroleum-based formulations for applications requiring higher toughness than neat PLA. Another significant advantage of combining ESOA with other polymeric materials is the improvement in thermal stability. This was demonstrated by Oprea et al. [11], who developed blends and subsequently films of ESOA and polyurethane acrylate that exhibited increased tensile strength and improved thermal stability, overcoming the typical limitations of polyurethanes in high-temperature resistance [12]. In order to extend the application of ESOA, this work investigated the possibility of combining this compound with a polymer of great interest, namely poly(N-isopropylacrylamide) (PNIPAAm), to develop innovative materials with modified properties compared to those obtained from NIPAAm and ESOA. It is worth underlining that the strategy of combining systems from renewable sources with those from non-renewable sources, such as PNIPAAm, can be seen as a way to reduce the impact of conventional materials from fossil sources on the one hand and to modify and improve the properties of materials produced from renewable sources on the other, an approach that was applied to various systems such as PLA/PMMA, PHB/PE, etc. [13–17].

The polymer we focused on our study, PNIPAAm, presents some drawbacks, especially in terms of mechanical properties [18]. This can be overcome by various approaches, including copolymerization, blending or combinations with other compounds that, if derived from renewable sources, make the formulation environmentally friendly. On the other hand, as previously mentioned, the development of novel formulations based on ESOA is an important goal, as it could allow an expansion of its applications. Given the hydrophobicity of ESOA, formulations based on this compound could enable the production of materials capable of retaining non-polar molecules, thus offering potential applications in water treatment. With this in mind, we designed a study in which we also used a very energy-efficient polymerization method, namely frontal polymerization. This polymerization technique was used in a series of studies to produce PNIPAAm-based hydrogels, in combination with a variety of polymer and non-polymer compounds, such as montmorillonite [19], polyvinylpyrrolidone [20], methylcellulose [21], polycaprolactone [22] and β-cyclodextrin [23], among others. Although these examples highlight the wide application of frontal polymerization in the preparation of PNIPAAm-based systems, it is important to underline that this method has not yet been used in the development of ESOA-based materials. The novelty of our work therefore relates to both the material development as well as to the preparation approach used for their synthesis. This work describes in particular the development of innovative systems based on ESOA and NIPAAm obtained by means of the frontal polymerization technique (Fig. 1). The thermal, mechanical and morphological properties of the materials were investigated as a function of the ratio between ESOA and NIPAAm. In addition, the swelling ratio of these systems was evaluated by testing it at different temperatures in MilliQ water to demonstrate the influence of the hydrophobic component and to allow a meaningful comparison with the swelling capacity of other PNIPAAm-based systems. Finally, with the aim of exploring a possible application of the formulations developed in the field of water treatment, and in particular in the removal of hydrophobic pollutants, the ability of the prepared samples to retain a hydrophobic molecule, namely Oil Red O, was investigated.

2. Materials and methods

2.1. Materials

Epoxidized Soybean Oil Acrylate (ESOA, with 4000 ppm hydroquinone monomethyl ether), N-isopropylacrylamide (NIPAAm, purity ≥ 97 %), dimetylsulfoxide (DMSO, purity ≥ 99 %), cyrene (purity ≥ 98.5 %), pentaerythritol tetraacrylate (PE-TA, with 350 ppm hydroquinone monomethyl ether), ammonium persulphate (APS, purity ≥ 98 %), trihexyl tetradecyl phosphonium chloride (TETDPC, purity ≥ 95 %), Oil Red O (solution 0.5 % in isopropanol), isopropanol (purity 69–71 %), were purchased from Sigma Aldrich® and used as received.

2.2. Sample preparation

For each sample, 5.0 g of monomer were used and the mass ratio between ESOA and NIPAAm was varied, as shown in Table 1. The samples were named according to their ESOA and NIPAAm concentration, e.g. ESOA60_NIP40 denotes the system with a ESOA and NIPAAm content of 60 and 40 wt% with respect to the total amount of monomer, respectively.

The radical initiator trihexyl tetradecyl phosphonium persulphate (TETDPPS) was prepared according to the procedure reported elsewhere [24] and used at a concentration of 5.0 mol% with respect to the molar concentration of acrylate groups. In the case of ESOA, the number of 3.4 acrylate groups per mole of triglyceride was taken as the basis for calculation.

To prepare the samples, ESOA and NIPAAm were mixed in a test tube with an inner diameter of 16 mm and a length of 100 mm in the presence of DMSO, which was identified as an optimal solvent, by using a mechanical stirrer. Once complete solubilization was achieved, the initiator was added, and the system was stirred for approximately one minute. Frontal polymerization was initiated by heating the outer wall of the upper part of the test tubes with a tin welder set at 450 °C.

The sample designated ESOA_100, which consists exclusively of ESOA, was prepared through a classical bulk polymerization due the low

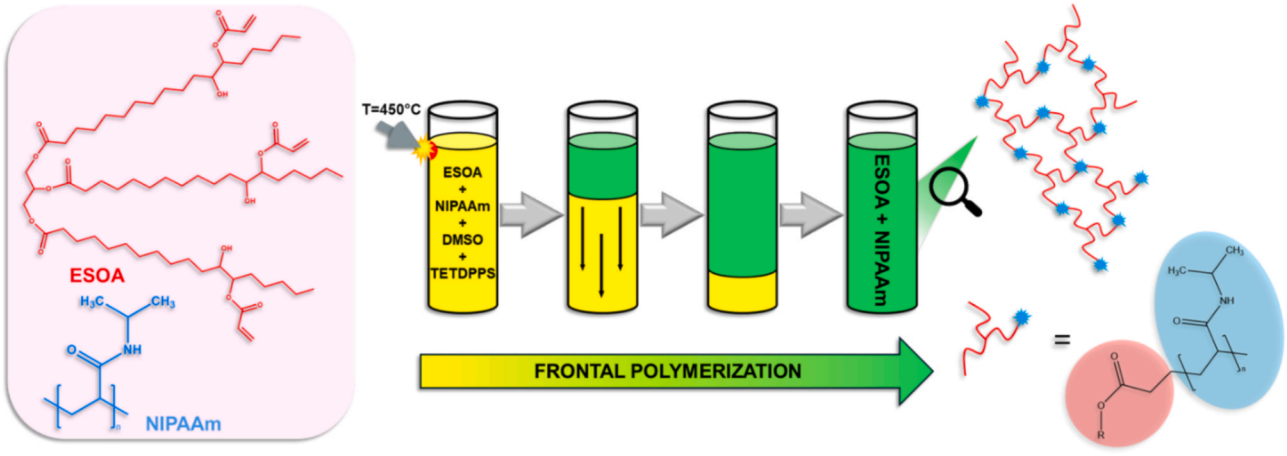

Fig. 1. Scheme of the formulation preparation.

Table 1
Characteristics of the prepared systems.

Sample code	ESOA [g]	NIPAAm [g]	TETDPPS [g]	DMSO [mL]	PE-TA [g]	Polymerization technique
ESOA_100	5.0	0.0	0.479	0.0	–	BP
ESOA90_NIP10	4.5	0.5	0.579	0.3	–	FP
ESOA80_NIP20	4.0	1.0	0.682	0.6	–	FP
ESOA70_NIP30	3.5	1.5	0.783	0.9	–	FP
ESOA60_NIP40	3.0	2.0	0.884	1.2	–	FP
ESOA50_NIP50	2.5	2.5	0.985	1.5	–	FP
ESOA40_NIP60	2.0	3.0	1.087	1.8	–	FP
ESOA30_NIP70	1.5	3.5	1.189	2.1	–	FP
ESOA20_NIP80	1.0	4.0	1.291	2.4	–	FP
ESOA10_NIP90	0.5	4.5	1.392	2.7	–	FP
NIP_100	0.0	5.0	1.488	3.0	–	FP
PETA_NIP	–	4.5	1.396	2.7	0.417	FP

BP = bulk polymerization, FP = frontal polymerization

reactivity of the monomer in question. Again, the radical initiator TETDPPS was used at a concentration of 5.0 mol%, based on the moles of acrylate groups, and the polymerization was carried out at a temperature of 80 °C.

Sample PETA_NIP was prepared by substituting ESOA with pentaerythritol tetraacrylate. The amount of PE-TA was chosen in order to maintain the same concentration of acrylate groups in moles as that of ESOA10_NIP90 sample, which allowed a meaningful comparison between the two systems.

2.3. Characterization

The frontal polymerization process was investigated with regard to the velocity of the reaction front (V_f) and the front temperature (T_{max}). The temperature (±10 °C) was recorded using a K-type thermocouple connected to a digital multimeter inserted into the reaction system at a depth of approximately 3 cm from the bottom of the test tubes used for sample preparation. The front velocity (± 0.05 cm/min) was determined by monitoring its position over time. The thermal characterization of the samples was performed using a Mettler Toledo differential scanning calorimeter (DSC1 STARe System®). The analyses were carried out between −100 and 200 °C, with a heating/cooling rate of ± 10 °C/min and an N_2 flow rate of 20 mL/min. Observation and examination of the thermograms enabled the acquisition of glass transition temperature (T_g) for the various formulations.

A Zeiss Supra 40 VP field emission scanning electron microscope, equipped with a backscattered electron detector, was employed for the morphological analysis of the samples. Prior to analysis, the samples were cryogenically fractured, immersed in liquid nitrogen, and covered with a thin layer of graphite using a Polaron E5100.

To determine the swelling ratio, square specimens of approximately 0.5 cm side length were taken from each sample. These were washed in MilliQ water for three days, changing the water every 24 h. They were then washed in toluene for a further three days, changing the solvent every 24 h. The specimens were then dried in a vacuum oven at room temperature until they reached a constant weight. The swelling ratio of the samples was quantified through testing in MilliQ water at temperatures ranging from 2 to 34 °C, with an increase of ca. 2–3 °C every 24 h.

The percentage swelling ratio (SR%) was then calculated using **Eq. (1)**:

$$SR(\%) = \frac{M_s - M_d}{M_d} \cdot 100 \quad (1)$$

Where M_s and M_d are the weight of the swollen sample and the dried sample, respectively. The reported data are an average of three measurements (reproducibility was about ± 10 %).

Gel fraction tests were carried out to determine the degree of cross-linking of the samples and thus the yield of the polymerization reaction. Square specimens with a side length of approximately 0.5 cm were cut from each sample, dried in a vacuum oven after the washing procedures described above, and weighed. The samples were then immersed in 3 mL anhydrous toluene for 24 h, dried in a vacuum oven and weighed again. The same procedure was repeated a second time and the percentage gel fraction (GF%) was calculated using **Eq. (2)**:

$$GF\% = \frac{M_{d,2}}{M_{d,1}} \cdot 100 \quad (2)$$

Where $M_{d,2}$ and $M_{d,1}$ are the weight of the dried sample after second and first washing respectively.

The same procedure was then repeated in MilliQ water. The reported data are an average of three measurements (reproducibility was about ± 10 %).

The mechanical properties of the samples were analysed at room temperature (T = 25 °C) using a dynamic mechanical analyser (DMA) TA-Q-800 instrument (TA Instruments), equipped with the TA Universal Analysis 2000 software. The samples were cut into squares with a side length of approximately 6.0 mm and a height of approximately 3.0 mm and subjected to dry and immersion compression tests employing the appropriate clamps. For the immersion compression tests, the specimens were placed in the clamp tank, which was filled with sufficient water to fully submerge the samples. The tests were conducted using a controlled force method with a force ramp from 0 to 18 N, with an increment of 1.0 N/min and a preload of 0.01 N. The elastic modulus was calculated at 3.0 % strain. For each sample three measures were performed, and the mean values were reported; the standard deviation was always below 5 %.

2.4. Retention tests

For the retention tests, square specimens of approximately 0.5 cm side length were excised from each sample. A solution of 0.5 % Oil Red O in isopropanol, which is commonly used to highlight lipids and water-insoluble substances, was used [25]. The dye was diluted 1:30 ratio in isopropanol and the specimens were immersed in 5.0 mL of this solution for 24 h. The supernatant was analysed using a Shimadzu® UV 1800 UV–Vis spectrometer. To quantify the amount of dye adsorbed by each sample, a calibration curve was constructed by measuring the absorbance relative to standard solutions at different dye concentrations at the characteristic wavelength of Oil Red O, *i.e.* 515 nm. **Equation (3)** was then applied:

$$Absorbance[a.u.] = 0.00913 \cdot Concentration[\mu g/mL] + 0.40835 \quad (3)$$

$$R^2 = 0.98396$$

3. Results and discussion

3.1. Study of the frontal polymerization parameters

Fig. 2 shows the trends of V_f, (Fig. 2a) and T_{max} (Fig. 2b) as a function of the NIPAAm concentration (expressed as a wt.% with respect to the total amount of the two compounds). The figures do not show data for ESOA_100 because it was obtained by batch polymerization only. Indeed, this is due to the balance between the heat developed by the polymerization involving the acrylic groups and that absorbed by the non-reactive part of the ESOA, which results in insufficient energy to sustain the polymerization front. Nevertheless, it is interesting to notice that as low as 10 wt% NIPAAm was sufficient to sustain the front propagation, allowing the preparation of very rich ESOA formulations by exploiting frontal polymerization.

The curves shown in Fig. 2 indicate that both parameters are strongly influenced by the NIPAAm concentration in the reaction mixture, with V_f and T_{max} showing a similar trend. In particular, it can be observed that V_f ranged from ≈ 0.5 cm/min for the sample with the lowest NIPAAm concentration, namely ESOA90_NIP10, to ≈ 1.8 cm/min for ESOA10_NIP90.

The variation of V_f as a function of NIPAAm amount was greater at the lower concentrations: for example, V_f doubles (from ≈ 0.5 cm/min to ≈ 1.0 cm/min) when the concentration increases from 10 to 20 %, while it reaches an almost constant value of 1.7 cm/min from ESOA40_NIP60. It can also be observed that the NIPAAm homopolymer has a lower V_f value than the samples based on the highest ESOA content. To explain these results, one must take into account that this sample was not cross-linked, and its polymerization front was characterized by the fingering phenomenon, in which, as described in the literature, some pieces of the denser polymer drip into the cold monomer, thereby removing heat from the propagating front and triggering bulk polymerization within the monomer itself [26]. As already mentioned, the same trend was observed for T_{max} as for V_f: the front temperature increased almost hyperbolically with increasing NIPAAm concentration, and a decrease in T_{max} due to fingering can be observed for NIP_100.

Finally, analysis of the values of V_f and T_{max} for the sample in which ESOA was replaced by the same molar amount of reactive acrylate groups of pentaerythritol tetraacrylate, PETA_NIP (**Fig. S1**), revealed that both V_f and T_{max} values were lower than that obtained for the corresponding system based on ESOA, demonstrating the lower reactivity of PE-TA compared to ESOA. This phenomenon can be explained by considering various parameters that may affect polymerization, e.g. the different viscosity of the reactive mixture, which can influence the diffusivity of the reagents and the specific reactivity due to the different chemical structure of ESOA and PE-TA [27].

3.2. Morphological analysis

Fig. 3 shows the FE-SEM micrographs of the cross-section of some of the prepared samples subjected to freeze-drying process, namely ESOA90_NIP10 (Fig. 3a), ESOA50_NIP50 (Fig. 3b), and ESOA10_NIP90 (Fig. 3c). These samples were selected as representative of the evolution of morphology depending on the composition of the reaction mixture.

Although the ESOA/NIPAAm-based samples did not exhibit a clear sponge-like morphology typical of hydrogels, the porosity/roughness increased with increasing NIPAAm content in the reaction mixture. This can be attributed to the presence of ESOA, which makes the material more compact and with a lower affinity for water. Indeed, these results must be taken into account to explain the properties of the systems as reported for other PNIPAAM-based materials, where both the degree of crosslinking and the strength were correlated with their morphology [22]. In addition, it should be highlighted that the morphological homogeneity of the ESOA/NIPAAm-based samples indicates a good compatibility between the two phases that compose the material after the polymerization reaction.

3.3. Thermal properties of the ESOA/NIPAAm systems

The systems prepared starting from neat ESOA (ESOA_100) and PNIPAAm (NIP_100) as well as the formulations based on both ESOA and NIPAAm were characterized in terms of their thermal properties using a differential scanning calorimeter. The resulting data are shown in Table 2, while DSC traces are given in the Supporting Information (**Fig. S2**).

In the second heating DSC trace, ESOA_100 exhibited a glass transition temperature (T_g) of 32 °C, thus demonstrating the typical thermal behaviour of an amorphous polymer. It was reported that the T_g of ESOA depends on the curing conditions and consequently on the degree of cross-linking. For example, Lebedevaite et al. [28] prepared a system of neat ESOA that exhibited a degree of cross-linking of 88 %, and a T_g of −4.5 °C, while Yang et al. [29] reported the development of an ESOA-based sample with a cross-linking density of 751 mol/m^3 and a T_g of 16 °C.

In the case of NIP_100, a T_g of 103 °C was observed, which is consistent with the value of linear non-crosslinked polymer [30]. The formulations containing ESOA and NIPAAm in different ratios exhibited a single T_g, which increased when the NIPAAm content was augmented at least up to a concentration of 40 wt%. Indeed, T_g ranged from 64 °C for ESOA90_NIP10 – a sample containing 10 wt% NIPAAm –, to 105 °C for that with 40 wt%, ESOA60_NIP40. The samples with higher NIPAAm concentration also had a single T_g characterized by values close to that of neat PNIPAAm, *i.e.*, around 103 °C. Indeed, the fact that the materials were characterized by a single T_g is evidence of a good compatibility

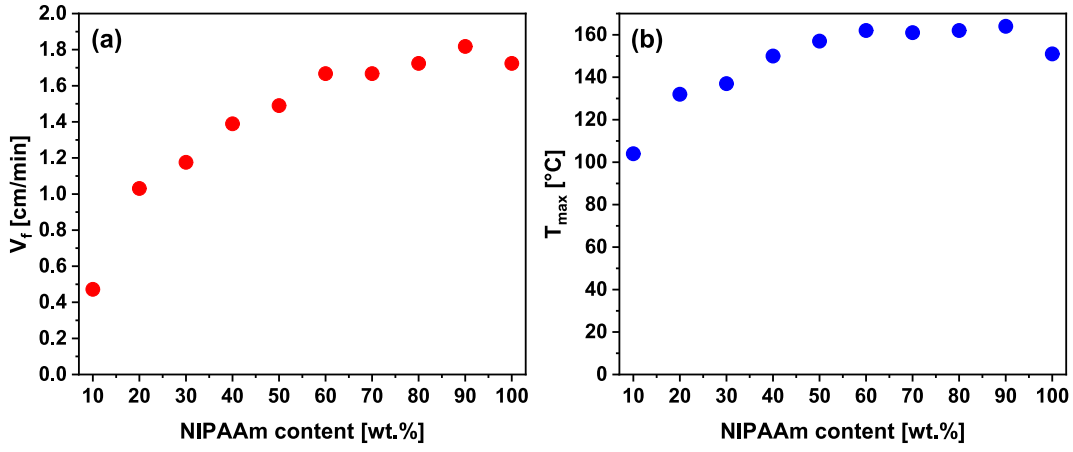

Fig. 2. (a) V_f and (b) T_{max} as a function of NIPAAm concentration for the ESOA/NIPAAm systems.

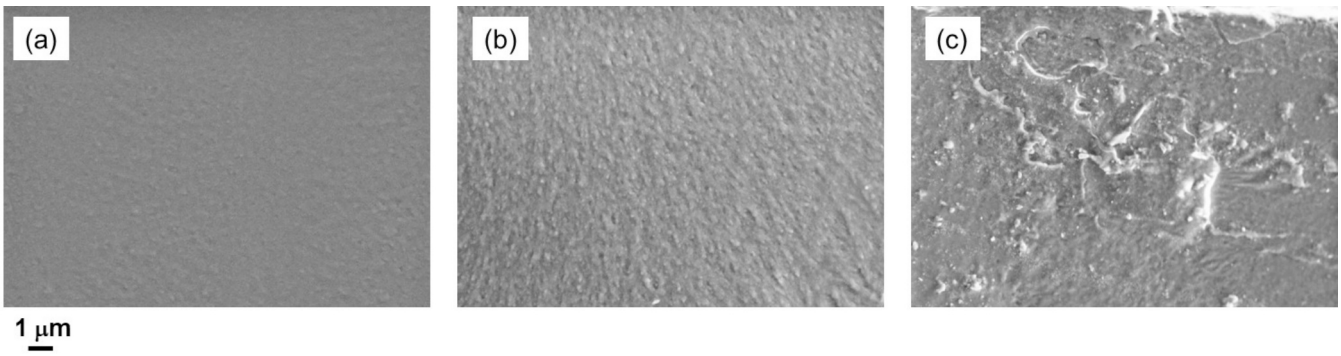

Fig. 3. FE-SEM micrographs: (a) ESOA90_NIP10, (b) ESOA50_NIP50 and (c) ESOA10_NIP90.

Table 2
T_g and gel fraction (GF) for samples based on neat ESOA (ESOA_100), neat NIPAAm (NIP_100) and the formulations ESOA/NIPAAm, and PETA_NIP.

Sample code	T_g [°C]	GF_w[a] [%]	GF_t[b] [%]
ESOA_100	32	99	98
ESOA90_NIP10	64	99	97
ESOA80_NIP20	94	99	97
ESOA70_NIP30	98	99	98
ESOA60_NIP40	105	99	98
ESOA50_NIP50	102	99	96
ESOA40_NIP60	102	99	96
ESOA30_NIP70	107	97	96
ESOA20_NIP80	106	97	97
ESOA10_NIP90	106	94	99
NIP_100	103	–	–
PETA_NIP	115	90	97

[a] GF_w measured in water at room temperature,
[b] GF_t measured in toluene at room temperature.

between the formulation components and that ESOA acts as a co-monomer/crosslinker in the crosslinking process, which probably favours the formation of a copolymer system within the network. Furthermore, the increase in T_g in the ESOA/NIPAAm-based samples compared to neat ESOA – a phenomenon that cannot be related to a change in the degree of crosslinking, as the samples exhibited a similar GF – suggests that the incorporation of NIPAAm into the network leads to a decrease in free volume. In contrast, the glass transition temperature of the samples with a high ESOA content showed a lower value compared to fully crosslinked PNIPAAm systems characterized by a T_g of about 130 °C [31,32], suggesting that the ESOA improve the free volume of the ESOA/NIPAAm network.

Finally, the glass transition temperature of PETA_NIP was found to be higher than that of the corresponding ESOA-based sample, being 115 and 106 °C for PETA_NIP and ESOA10_NIP90, respectively, which is probably due to the different mobility of the two chemical structures.

3.4. Gel fraction of the ESOA/NIPAAm systems

In order determine the formation of a three-dimensional network in the NIPAAm/ESOA system, gel fraction (GF) tests were carried out. After checking the solubility of the starting reagents, water and toluene were identified as suitable solvents for carrying out these tests. Indeed, water is able to solubilize the residual unreacted NIPAAm, while toluene can dissolve the unreacted ESOA. The results of the gel fraction tests are given in Table 2 as a function of NIPAAm concentration relative to the total amount of monomers in the systems.

The gel fraction tests carried out in water evidenced that samples containing up to 60 wt% ESOA exhibited a degree of cross-linking of almost 100 %, which decreased to 94 % only for the sample based on the highest content of NIPAAm, namely ESOA10_NIP90.

The GF values in toluene were also high, ranging from 99 % in systems with the highest NIPAAm content to 96 % in those with lowest amounts, showing that both compounds, NIPAAm and ESOA, were involved in network formation. Moreover, the gel fraction values found are consistent with those of other materials composed of cross-linked PNIPAAm or ESOA described in the literature [33,34]. However, it is worth underling that similar GF values were obtained using thermal curing, which took much longer than frontal polymerization approach. For example, Chuang et al. [35] reported the development of hydrogels based on NIPAAm and N-methylol acrylamide prepared by redox polymerization, finding a GF close to 90 % after one hour of thermal curing at 110 °C. At the same time, Paramarta et al. [36] reported the development of thermoset coatings based on acrylated epoxidized soybean oil and an amine crosslinker, prepared via aza-Michael reaction, which achieved cross-linking of approximately 93 % with a curing time of 45 min at 80 °C. These results clearly demonstrate the effectiveness of the preparation method used in our work, which is able to activate the formation of a network in a very short time, on the order of seconds.

3.5. Swelling properties of the ESOA/NIPAAM systems

The swelling properties of the ESOA/NIPAAm-based formulations were investigated by testing in MilliQ water, as this is the usual medium for analyzing the swelling capacity of PNIPAAm-based systems [37,38].

Fig. 4 shows the swelling ratio % (SR%) at room temperature (25 °C) as a function of formulation composition. It can be seen that SR% was

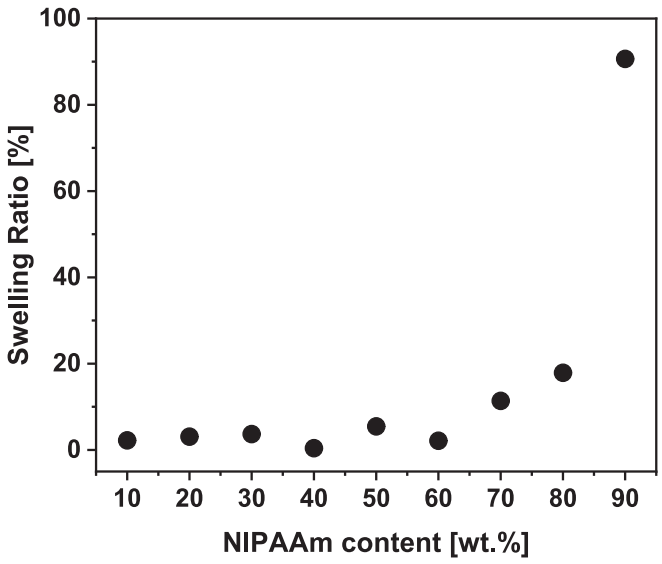

Fig. 4. SR% as a function of NIPAAm concentration in ESOA/NIPAAm copolymer systems.

strongly influenced by the presence of ESOA in the system, with this parameter decreasing as the amount of ESOA increases. There are two main effects to consider: cross-linking density and hydrophobicity. The first aspect is that ESOA acts as a cross-linker of NIPAAm and thus influences the formulation cross-linking density, while the second aspect is that ESOA is a molecule that has a highly hydrophobic central part due to the long alkyl chains. Both factors can contribute to an increase in the hydrophobicity of the system as the amount of ESOA in the reagent mixture increases. At NIPAAm concentrations up to 60 wt%, the SR% resulted to be less than 10 %, indicating that the samples were highly hydrophobic and cross-linked, as the long alkyl chains of ESOA, forming a hydrophobic environment, and the tight mesh of the polymer network prevented water molecules from penetrating and swelling the material.

From ESOA70_NIP30, SR% increased significantly and doubled compared to ESOA40_NIP60, indicating an increase in both the hydrophilicity and mesh size. The sample with the highest NIPAAm concentration (ESOA10_NIP90) was the only one with a high swelling degree (91 %). Indeed, in the synthesis of hydrogels, NIPAAm is usually crosslinked using amounts of crosslinkers that do not exceed 5 mol% to ensure good swelling of the final material. For example, a swelling ratio of 650 % was achieved with 5 mol% N,N'-bisacrylamide [39], while with 2.5 mol% triethylenglycoldimethacrylate (TGDMA) SR% was 750 [40].

Thus, we used ESOA in our formulations in amounts exceeding the typical value of NIPAAm crosslinkers, reaching almost 80 mol%. As already underlined, this justifies the high degree of crosslinking and the low affinity of the produced systems for water uptake. Nevertheless, the results obtained show: i) the reactivity of ESOA under the applied conditions, ii) the possibility of adjusting the swelling ratio by changing the ESOA content in the reaction mixture and iii) the fact that this compound has a dual function: as a co-monomer, as shown by the DSC results, and as a cross-linker. With regard to the latter aspect, it should be underlined that PNIPAAm-based formulations and copolymers usually use monomers with a single functional group, such as poly(N-isopropylacrylamide-co-acrylic acid)-based materials [41,42], so that a crosslinker must be added. The effect of ESOA structure also becomes clear when comparing the behaviour of ESOA10_NIP90 with PETA_NIP, which had an SR% of 91 and 287, respectively. As mentioned above, it can be inferred that the peculiar chemical structure of ESOA, which consists of long alkyl chains different from those of PE-TA, may affect the hydrophobicity of the resulting material and thus reduce its tendency to adsorb water.

In our study, the trend of SR% as a function of temperature was also investigated to verify the effect of ESOA on the lower critical solution temperature (LCST), which represents a typical feature of PNIPAAm. Indeed, the above temperature, which is about 32–33 °C in the neat sample [43], corresponds to the temperature at which the polymer undergoes a coil to globule transition. As shown in **Fig. S3**, the concentration of ESOA in the formulation at compositions up to 50 wt% was high enough to completely neutralize the effect of NIPAAm: the materials absorbed only very small amounts of water (average SR% < 10 %), and temperature had no effect on this parameter. In the case of ESOA40_NIP60, an increase in swelling was observed at the lowest temperature (SR% $= 25$ at 2 °C) but the LCST could not be determined yet (Fig. 5).

For samples with NIPAAm concentrations of 70 wt% and more, a clear dependence of the SR% on temperature can be observed, and two regions below and above the LCST can be identified, in which the polymer is in a swollen and unswollen state. In contrast to NIPAAm homopolymer hydrogels [40,44,45], the LCST for the above samples, is not sharp: the transition from coil to globule was hindered by the ESOA chains and occurred in a wider temperature range. Therefore, we decided to consider the point where the SR% variation reached the maximum slope to evaluate the LCST, finding that the amount of ESOA had a strong influence on the LCST as it moved to lower values with increasing the ESOA concentration.

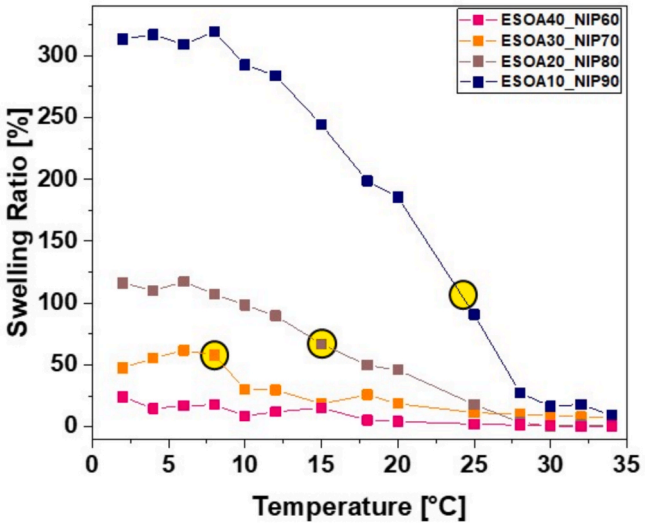

Fig. 5. SR% as a function of temperature for some representative samples of the series. For ESOA30_NIP70, ESOA20_NIP80 and ESOA10_NIP90, the lower critical solution temperature is indicated with yellow circles. (For interpretation of the references to colour in this figure legend, the reader is referred to the web version of this article.)

Specifically, the LCST was found to decrease from 24, to 15 to 8 °C when the ESOA concentration increased from 10 wt% (ESOA10_NIP90) to 20 wt% (ESOA20_NIP80) to 30 wt% (ESOA30_NIP70). Together with the LCST, the SR% of the polymers also changed at low temperatures: it increased significantly by increasing NIPAAm content. For example, the SR% values at 2 °C in the samples containing 50, 60, 70, 80 and 90 wt% NIPAAm, were 5, 24, 47, 116 and 313, respectively. To explain the behaviours described above, one must consider that the LCST phenomenon is determined by interactions leading to an attraction between polymer-water and polymer–polymer, where structural factors that increase polymer-water interactions lead to an increase in LCST, while an increase in polymer–polymer interactions decreases the value of LCST [46]. In the case of ESOA/NIPAAm-based systems, it is therefore possible to infer that the peculiar chemical structure of ESOA, together with its inherent hydrophobicity, reduces the specific interactions between the final material and water while favouring the interactions within the polymer network, thus reducing the LCST value.

3.6. *Mechanical properties of the ESOA/NIPAAm systems*

The mechanical properties of the developed formulations were studied by compression tests on swollen samples, both immersed and non-immersed in water. It is worth underling that this method was chosen as it allows to avoid the problems associated with tensile tests for PNIPAAm-based materials, which are mainly due to noisy measurements caused by the possible disruption of the generally soft samples, imperfect clamping and difficult redistribution of water within the specimens [47,48].

Table 3 shows the values of the compression modulus (E) for the ESOA/NIPAAm systems. The compression was evaluated on swollen samples, both immersed and non-immersed in water.

In particular, for the samples containing the highest amount of ESOA, the experiments carried out by compression without submersion yielded moduli that were much larger than those obtained by measurements with compression under immersion. It is noteworthy that in the case of ESOA90_NIP10, E decreased from 22 MPa to 2.3 MPa for compression and submersion compression tests, respectively. These results can be attributed to the plasticizing effect of water, which is greater when compression tests are performed on materials immersed in this medium, justifying the lower value of the modulus for the samples

Table 3
Elastic moduli at 3 % of strain carried out with DMA submersion compression and compression test.

Sample Code	Elastic Modulus[a] [MPa] [b]	Elastic Modulus [MPa] [b]
ESOA90_NIP10	2.3	22
ESOA80_NIP20	2.2	3.5
ESOA70_NIP30	1.7	3.0
ESOA60_NIP40	0.61	0.38
ESOA50_NIP50	0.46	0.19
ESOA40_NIP60	0.35	0.12
ESOA30_NIP70	0.32	0.12
ESOA20_NIP80	0.14	0.052
ESOA10_NIP90	0.030	0.028
PETA_NIP	0.011	0.021

[a] Submersion compression,
[b] the standard deviation was always below 5 %.

subjected to submersion compression. Despite this difference, the data for both types of measurements show a clear dependence of E on the composition of the formulation, with the above parameter decreasing as the ESOA content in the formulation diminishes. Indeed, as already mentioned, the systems become more hydrophilic as the ESOA content decreases, which increases the plasticizing effect of the water in the network, a phenomenon that contributes to the decrease in modulus.

It is difficult to compare the data obtained with those reported in the literature, as the mechanical properties of PNIPAAm-based materials are highly dependent on a number of parameters such as the measurement conditions, cross-linking state, etc [18]. Nevertheless, the material with the highest NIPAAm content, namely ESOA10_NIP90, was found to have a modulus consistent with the values reported in the literature for neat PNIPAAm hydrogel, which are in the range of 10–20 KPa [48,49]. In our materials, a relevant increase in modulus occurred in the sample based on 70 wt% ESOA, as E increased from 0.38 to 3.0 MPa in the case of compression tests and from 0.61 to 1.7 MPa in immersion compression tests in the case of ESOA60_NIP40 and ESOA70_NIP30, respectively. Systems consisting of 90 % ESOA, ESOA90_NIP10, exhibited a modulus that even reached 22 MPa. This result shows the formation of extremely stiff materials, but it is relevant to underline that the values obtained with lower amounts of ESOA, such as those based on 20 and 30 wt% ESOA, are also extremely interesting, as they achieved moduli comparable to those reported for composite/nanocomposite materials combining PNIPAAm with systems such as graphene oxide and clays [50,51]. Indeed, our formulations offer several advantages, as ESOA not only fulfils a dual function as a co-monomer and cross-linker but is also a compound from renewable sources that does not suffer from dispersion problems, as is the case with materials based on a mixture of inorganic (nano-)fillers. Finally, when comparing PETA_NIP with the analogous ESOA10_NIP90, the following can be stated: in the test without immersion, the modulus is higher for the sample cross-linked with ESOA, as the water content in the polymer is low (see the SR% values in Fig. 3). For the samples immersed in water, the modulus is higher for the sample with PE-TA, a phenomenon that is probably due to the combined effect of the greater mobility of the ESOA chains and the plasticizing effect of the medium. Indeed, for the PE-TA cross-linked sample, the plasticizing effect of immersion is less evident because the non-immersed sample, which is much more hydrophilic, already contains a high quantity of water.

3.7. Retention tests

Retention tests were performed using Oil Red O (ORO), a non-polar organic dye used for the histological staining of hydrophobic lipids and belonging to a class of highly lipophilic azo dyes commonly known as Sudans [52,53]. It is worth underlining that Sudan class dyes were used to colour soybean oil and its derivatives to perform oil repellency tests [54], oil/water separation experiments [55] and analysis on wettability behaviour [56]. The choice to use ORO was based on the aim to investigate the effect of the hydrophobic nature of our formulation, related to the presence of ESOA, on the adsorption capacity of water-insoluble molecules [25]. Although the ability of these vegetable oils to interact with azo dyes is well-known, the retention capacity of the above dyes in ESOA-based systems has never been investigated. In order to obtain a more comprehensive understanding of the results obtained, the samples were subjected to swelling tests at room temperature in isopropanol, the solvent used to dissolve the dye and thus to perform the retention tests. The swelling ratios and the amount of dye adsorbed by the prepared samples are summarized in Table 4, while Fig. 6 shows the amount of dye retained by the samples based on ESOA and NIPAAm.

The swelling ratio (SR%) data in isopropanol showed almost constant values (around 30 %) for samples with an ESOA concentration of up to 60 %, while for the samples prepared with lower amounts the SR tended to increase until the value of 258 % was reached. These results can be interpreted taking into account the fact that, as discussed for swelling in water, for materials with high amounts of ESOA, the predominant effect related to the hydrophobicity of the system reduces its affinity for the swelling medium. In contrast, it was reported in the literature that the swelling of NIPAAm-based systems in isopropanol increases with increasing alcohol content in the mixture with water [57], indicating an affinity of the polymer for this medium, as found in the samples based on a higher NIPAAm content. As far as the retained dye values are concerned, the behavior of the developed materials is extremely peculiar. Indeed, up to a concentration of 60 wt% ESOA, the amount of dye absorbed was ca. 500 μg/g. The behavior of the above formulations can be explained considering that, although the swelling values were low, the affinity for the dye was mainly determined by the hydrophobic component of the system. It is surprising that the formulation ESOA50_NIP50 had about twice the retention capacity, which corresponds to 900 μg/g. For the samples with an ESOA concentration of less than 50 wt%, this capacity decreases from approx. 450 μg/g to approx. 60 μg/g. From this it can be concluded that, despite the high swelling ratio, the affinity for the dye decreases with the increase in the amount of NIPAAm, which represents the hydrophilic portion of the formulation. The sample ESOA50_NIP50, which is characterized by the highest retention capacity, deserves a more detailed comment. This system represents an optimal compromise between the hydrophobicity of ESOA, which allowed an effective interaction with ORO, and the high degree of swelling, due to the presence of NIPAAm in the system, which facilitates the adsorption of solvent and improves the ability to interact with the dye. Furthermore, these results show the specific influence of the degree of swelling on the retention capacity of the material. Since the SR% clearly depends on the type of medium used, it can be deduced that retention of the system can also be tuned by changing the environment with which the material comes into contact.

These results, although related to a single compound, are very interesting considering that PNIPAAm-based materials – generally having a great ability to retain both positively and negatively charged dyes in aqueous solutions [58–61] – cannot interact with highly hydrophobic molecules such as ORO and encourage exploring the

Table 4
Amount of retained Oil Red O and swelling ratio in isopropanol for ESOA/NIPAAm systems.

Sample code	Retained dye [μg/g]	SR% in isopropanol [%]
ESOA90_NIP10	489 ± 79	31
ESOA80_NIP20	449 ± 111	33
ESOA70_NIP30	536 ± 26	35
ESOA60_NIP40	507 ± 51	35
ESOA50_NIP50	931 ± 69	178
ESOA40_NIP60	449 ± 19	201
ESOA30_NIP70	425 ± 28	231
ESOA20_NIP80	199 ± 24	241
ESOA10_NIP90	61 ± 22	258

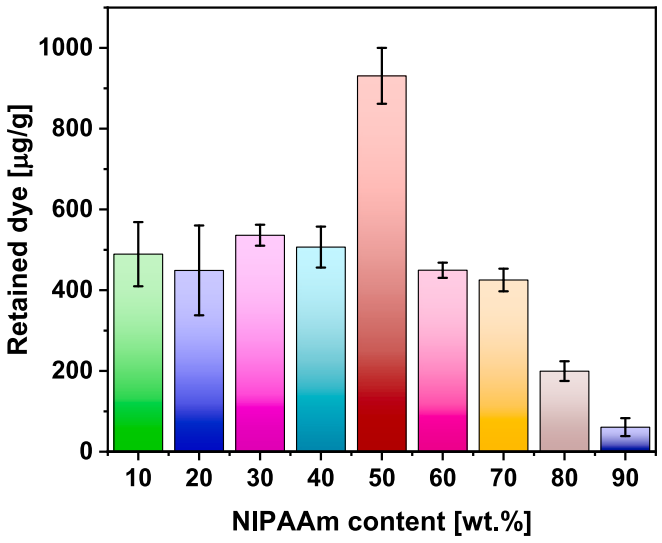

Fig. 6. Retained dye as a function of NIPAAm concentration in ESOA/NIPAAm systems.

versatility of the materials towards other molecules as well their biodegradability in a future research. Considering the latter aspect, it is important to underline that although biodegradability and environmental impact will be the subject of a future work, materials based on neat ESOA and NIPAAm, the two components of our formulations, were evaluated in several works demonstrating biocompatibility and degradability without release of any toxic compounds [62–68]. Therefore, it is possible to conclude that the optimal formulation developed possesses characteristics not shared with other NIPAAm-based systems, not only for the ability to interact with hydrophobic compounds and for the bio-based nature of one of the two components, but also in terms of mechanical properties.

4. Conclusions

In this work, the possibility of exploiting a bio-based compound, namely ESOA, in polymer formulations prepared by a free radical process using the frontal polymerization technique was demonstrated. In particular, the above polymerization method was effectively applied to obtain formulations with different ESOA/NIPAAm ratios, also based on high ESOA contents (up to 90 %), which were found to be fully crosslinked. The prepared systems, in which ESOA fulfill a dual function as co-monomer and as crosslinker, were homogeneous, phenomenon that can be attributed to possible exchange reactions that could lead to the formation of copolymer systems that increase the compatibility between the phases. Indeed, the combination of ESOA with NIPAAm in the reactive process made it possible to obtain materials whose properties depend on the ratio between the components of the mixture. In particular, it was found that the degree of swelling decreased with increasing ESOA content in the formulation, while the mechanical properties increased significantly in systems with high ESOA content, improving one of the main problems associated with the application of PNIPAAm. Finally, a formulation characterized by the right combination of swelling and hydrophobicity was found, allowing to maximize the adsorption capacity of hydrophobic compounds – a property not present in normal PNIPAAm-based systems. The properties of the developed materials, the renewable source for one of the two components as well as the applied polymerization method make the systems promising in terms of their application and large-scale development.

CRediT authorship contribution statement

Martina Cozzani: Writing – original draft, Visualization, Validation, Investigation, Data curation. **Daniele Nuvoli:** Writing – original draft, Validation, Methodology, Investigation, Data curation, Conceptualization. **Alberto Mariani:** Writing – review & editing, Validation, Resources, Methodology, Conceptualization. **Orietta Monticelli:** Writing – review & editing, Validation, Supervision, Methodology, Funding acquisition, Conceptualization.

Declaration of competing interest

The authors declare that they have no known competing financial interests or personal relationships that could have appeared to influence the work reported in this paper.

Appendix A. Supplementary data

Front velocity and front temperature for ESOA10_NIP90 and PETA_NIP, DSC traces, second heating for the prepared formulations, SR % as a function of temperature for the prepared formulations, comparison between SR% as a function of temperature of ESOA50_NIP50 and ESOA10_NIP90. Supplementary data to this article can be found online at https://doi.org/10.1016/j.eurpolymj.2025.114084.

Data availability

Data will be made available on request.

References

[1] C. Maraveas, Production of sustainable and biodegradable polymers from agricultural waste, Polymers 12 (2020) 1127, https://doi.org/10.3390/polym12051127.
[2] T. Välsänen, A. Haapala, R. Lappalainen, L. Tomppo, Utilization of agricultural and forest industry waste and residues in natural fiber-polymer composites: a review, Waste Manag. 54 (2016) 62–73, https://doi.org/10.1016/j.wasman.2016.04.037.
[3] M.K. Thakur, V.K. Thakur, R.K. Gupta, A. Pappu, Synthesis and applications of biodegradable soy based graft copolymers: a review, ACS Sustain. Chem. Eng. 4 (2016) 1–17, https://doi.org/10.1021/acssuschemeng.5b01327.
[4] S.M. Danov, O.A. Kazantsev, A.L. Esipovich, A.S. Belousov, A.E. Rogozhin, E. A. Kanakov, Recent advances in the field of selective epoxidation of vegetable oils and their derivatives: a review and perspective, Catal. Sci. Technol. 7 (2017) 3659–3675, https://doi.org/10.1039/C7CY00988G.
[5] B.K. Sharma, Z. Liu, A. Adhvaryu, S.Z. Erhan, One-pot synthesis of chemically modified vegetable oils, J. Agric. Food Chem. 56 (2008) 3049–3056, https://doi.org/10.1021/jf073070z.
[6] S.Z. Erhan, B.K. Sharma, Z. Liu, A. Adhvaryu, Lubricant base stock potential of chemically modified vegetable oils, J. Agric. Food Chem. 56 (2008) 8919–8925, https://doi.org/10.1021/jf801463d.
[7] R.C. Amos, M. Kuska, J. Mesnager, M. Gauthier, Thermally induced maleation of soybean and linseed oils: from benchtop to pilot plant, Ind. Crop. Prod. 166 (2021) 113504, https://doi.org/10.1016/j.indcrop.2021.113504.
[8] F. Habib, M. Bajpai, Synthesis and characterization of acrylated epoxidized soybean oil for UV cured coatings, Chem. Chem. Technol. 5 (2011) 317–326, https://doi.org/10.23939/chcht05.03.317.
[9] D. Behera, A.K. Banthia, Synthesis, characterization, and kinetics study of thermal decomposition of epoxidized soybean oil acrylate, J. Appl. Polym. Sci. 109 (2008) 2583–2590, https://doi.org/10.1002/app.28350.
[10] S.C. Mauck, S. Wang, W. Ding, B.J. Rohde, C.K. Fortune, G. Yang, S.-K. Ahn, M. L. Robertson, Biorenewable tough blends of polylactide and acrylated epoxidized soybean oil compatibilized by a polylactide star polymer, Macromolecules 49 (2016) 1605–1615, https://doi.org/10.1021/acs.macromol.5b02613.
[11] S. Oprea, Properties of polymer networks prepared by blending polyester urethane acrylate with acrylated epoxidized soybean oil, J. Mater. Sci. 45 (2010) 1315–1320, https://doi.org/10.1007/s10853-009-4084-5.
[12] S.-H. Liu, M.-Y. Shen, C.-F. Kuan, H.-C. Kuan, C.-Y. Ke, C.-L. Chiang, Improving thermal stability of polyurethane through the addition of hyperbranched polysiloxane, Polymers 11 (2019) 697, https://doi.org/10.3390/polym11040697.
[13] N.F. Mazuki, Y. Nagao, M.Z. Kufian, A.S. Samsudin, The influences of PLA into PMMA on crystallinity and thermal properties enhancement-based hybrid polymer in gel properties, Mater. Today 49 (2022) 3105–3111, https://doi.org/10.1016/j.matpr.2020.11.037.
[14] T. Tamiya, X. Cui, Y.-I. Hsu, T. Kanno, T.-A. Asoh, H. Uyama, Enhancement of interfacial adhesion in immiscible polymer blend by using a graft copolymer synthesized from propargyl-terminated poly(3-hydroxybutyrate-co-3-hydroxyhexanoate), Eur. Polym. J. 130 (2020) 109662, https://doi.org/10.1016/j.eurpolymj.2020.109662.

[15] G. Biresaw, C.J. Carriere, Compatibility and mechanical properties of blends of polystyrene with biodegradable polyesters, Compos. A Appl. Sci. Manuf. 35 (2004) 313–320, https://doi.org/10.1016/j.compositesa.2003.09.020.

[16] W. Shujun, Y. Jiugao, Y. Jinglin, Preparation and characterization of compatible thermoplastic starch/polyethylene blends, Polym. Degrad. Stab. 87 (2005) 395–401, https://doi.org/10.1016/j.polymdegradstab.2004.08.012.

[17] G.A.D. Burlein, M.C.G. Rocha, Mechanical and morphological properties of LDPE/PHB blends filled with castor oil pressed cake, Mater. Res. 17 (2014) 97–105, https://doi.org/10.1590/S1516-14392013005000196.

[18] M.A. Haq, Y. Su, D. Wang, Mechanical properties of PNIPAM based hydrogels: a review, Mater. Sci. Eng. C 70 (2017) 842–855, https://doi.org/10.1016/j.msec.2016.09.081.

[19] Q. Feng, X. Chen, Y.-Q. Zhao, S.-S. Hu, Z.-W. Xia, Q.-Z. Yan, Preparation of poly(N-isopropylacrylamide)/montmorillonite composite hydrogel by frontal polymerization, Colloid Polym. Sci. 295 (2017) 883–890, https://doi.org/10.1007/s00396-017-4066-0.

[20] Q. Feng, Y. Zhao, H. Li, Y. Zhang, X. Xia, Q. Yan, Frontal polymerization and characterization of interpenetrating polymer networks composed of poly(N-isopropylacrylamide) and polyvinylpyrrolidone, Colloid Polym. Sci. 296 (2018) 165–172, https://doi.org/10.1007/s00396-017-4215-5.

[21] A. Mariani, L. Nuvoli, D. Sanna, V. Alzari, D. Nuvoli, M. Rassu, G. Malucelli, Semi-interpenetrating polymer networks based on crosslinked poly(N-isopropyl acrylamide) and methylcellulose prepared by frontal polymerization, J. Polym. Sci. A Polym. Chem. 56 (2017) 437–443, https://doi.org/10.1002/pola.28914.

[22] G. Damonte, M. Cozzani, D. Di Lisa, L. Pastorino, A. Mariani, O. Monticelli, Mechanically-reinforced biocompatible hydrogels based on poly(N-isopropylacrylamide) and star-shaped polycaprolactones, Eur. Polym. J. 195 (2023) 112239, https://doi.org/10.1016/j.eurpolymj.2023.112239.

[23] D. Sanna, V. Alzari, D. Nuvoli, L. Nuvoli, M. Rassu, V. Sanna, A. Mariani, β-Cyclodextrin-based supramolecular poly(N-isopropylacrylamide) hydrogels prepared by frontal polymerization, Carbohydr. Polym. 166 (2017) 249–255, https://doi.org/10.1016/j.carbpol.2017.02.099.

[24] A. Mariani, D. Nuvoli, V. Alzari, M. Pini, Phosphonium-based ionic liquids as a new class of radical initiators and their use in gas-free frontal polymerization click, Macromolecules 41 (2008) 5191–5196, https://doi.org/10.1021/ma800610g.

[25] A. Mehlem, C.E. Hagberg, L. Muhl, U. Eriksson, A. Falkevall, Imaging of neutral lipids by oil red O for analyzing the metabolic status in health and disease, Nat. Protoc. 8 (2013) 1149–1154, https://doi.org/10.1038/nprot.2013.055.

[26] B.A. Suslick, J. Hemmer, B.R. Groce, K.J. Stawiasz, P.H. Geubelle, G. Malucelli, A. Mariani, J.S. Moore, J.A. Pojman, N.R. Sottos, Frontal polymerizations: from chemical perspectives to macroscopic properties and applications, Chem. Rev. 123 (2023) 3237–3298, https://doi.org/10.1021/acs.chemrev.2c00686.

[27] J.A. Pojman, V.M. Ilyashenko, A.M. Khan, Free-radical frontal polymerization: self-propagating thermal reaction waves, J. Chem. Soc. Faraday Trans. 92 (1996) 2825–2837, https://doi.org/10.1039/FT9969202825.

[28] M. Lebedevaite, J. Ostrauskaite, E. Skliutas, M. Malinauskas, Photoinitiator free resins composed of plant-derived monomers for the optical μ-3D printing of thermosets, Polymers 11 (2019) 116, https://doi.org/10.3390/polym11010116.

[29] Y. Yang, M. Shen, X. Huang, H. Zhang, S. Shang, J. Song, Synthesis and performance of a thermosetting resin: Acrylated epoxidized soybean oil curing with a rosin-based acrylamide, J. Appl. Polym. Sci. 134 (2016) 44545, https://doi.org/10.1002/app.44545.

[30] R.G. Sousa, W.F. Magalhães, R.F.S. Freitas, Glass transition and thermal stability of poly(N-isopropylacrylamide) gels and some of their copolymers with acrylamide, Polym. Degrad. Stab. 61 (1998) 275–281, https://doi.org/10.1016/S0141-3910(97)00209-7.

[31] M. Ito, T. Ishizone, Synthesis of well-defined block copolymers containing poly(N-isopropylacrylamide) segment by anionic block copolymerization of N-methoxylmethyl-N-isopropylacrylamide, Des. Monomers Polym. 7 (2004) 11–24, https://doi.org/10.1163/156855504322890016.

[32] X.-Z. Zhang, D.-Q. Wu, C.-C. Chu, Synthesis, characterization and controlled drug release of thermosensitive IPN-PNIPAAm hydrogels, Biomater 25 (2004) 3793–3805, https://doi.org/10.1016/j.biomaterials.2003.10.065.

[33] U. Gulyuz, O. Okay, Self-healing poly(N-isopropylacrylamide) hydrogels, Eur. Polym. J. 72 (2015) 12–22, https://doi.org/10.1016/j.eurpolymj.2015.09.002.

[34] S.-S. Kim, H. Ha, C.J. Ellison, Soybean oil-based thermoset films and fibers with high biobased carbon content via thiol-ene photopolymerization, ACS Sustain. Chem. Eng. 6 (2018) 8364–8373, https://doi.org/10.1021/acssuschemeng.8b00435.

[35] W.-J. Chuang, W.-Y. Chiu, H.-J. Tai, Thermally crosslinkable poly(N-isopropylacrylamide) copolymers: Synthesis and characterization of temperature-responsive hydrogel, Mater. Chem. Phys. 134 (2012) 1208–1213, https://doi.org/10.1016/j.matchemphys.2012.04.030.

[36] A. Paramarta, D.C. Webster, The exploration of Michael-addition reaction chemistry to create high performance, ambient cure thermoset coatings based on soybean oil, Prog. Org. Coat. 108 (2017) 59–67, https://doi.org/10.1016/j.porgcoat.2017.04.004.

[37] S. Gallagher, L. Florea, K.J. Fraser, D. Diamond, Swelling and shrinking properties of thermo-responsive polymeric ionic liquid hydrogels with embedded linear pNIPAAM, Int. J. Mol. Sci. 15 (2014) 5337–5349, https://doi.org/10.3390/ijms15045337.

[38] L. Yang, L. Sun, Y. Sun, G. Qiu, X. Fan, Q. Sun, G. Lu, Engineering thermoresponsive poly(N-isopropylacrylamide)-based films with enhanced stability and reusability for efficient bone marrow mesenchymal stem cell culture and harvesting, Molecules 29 (2024) 4481, https://doi.org/10.3390/molecules29184481.

[39] S. Scognamillo, V. Alzari, D. Nuvoli, J. Illescas, S. Marceddu, A. Mariani, Thermoresponsive super water absorbent hydrogels prepared by frontal polymerization of N-isopropyl acrylamide and 3-sulfopropyl acrylate potassium salt, J. Polym. Sci. A Polym. Chem. 49 (2011) 1228–1234, https://doi.org/10.1002/pola.24542.

[40] V. Alzari, O. Monticelli, D. Nuvoli, J.M. Kenny, A. Mariani, Stimuli responsive hydrogels prepared by frontal polymerization, Biomacromolecules 10 (2009) 2672–2677, https://doi.org/10.1021/bm900605y.

[41] X. Gao, Y. Cao, X. Song, Z. Zhang, C. Xiao, C. He, X. Chen, pH- and thermo-responsive poly(N-isopropylacrylamide-co-acrylic acid derivative) copolymers and hydrogels with LCST dependent on pH and alkyl side groups, J. Mater. Chem. B 1 (2013) 5578–5587, https://doi.org/10.1039/C3TB20901F.

[42] Y. Pei, J. Chen, L. Yang, L. Shi, Q. Tao, B. Hui, J. Li, The effect of pH on the LCST of poly(N-isopropylacrylamide) and poly(N-isopropylacrylamide-co-acrylic acid), J. Biomater. Sci. Polym. Ed. 15 (2004) 585–594, https://doi.org/10.1163/156856204323046852.

[43] R. Pelton, Poly(N-isopropylacrylamide) (PNIPAM) is never hydrophobic, J. Colloid Interface Sci. 348 (2010) 673–674, https://doi.org/10.1016/j.jcis.2010.05.034.

[44] V. Alzari, A. Mariani, O. Monticelli, L. Valentini, D. Nuvoli, M. Piccinini, S. Scognamillo, S. Bittolo Bon, J. Illescas, Stimuli-responsive polymer hydrogels containing partially exfoliated graphite, J. Polym. Sci. A Polym. Chem. 48 (2010) 5375–5381, https://doi.org/10.1002/pola.24341.

[45] V. Alzari, D. Nuvoli, S. Scognamillo, M. Piccinini, E. Gioffredi, G. Malucelli, S. Marceddu, M. Sechi, V. Sanna, A. Mariani, Graphene-containing thermoresponsive nanocomposite hydrogels of poly(N-isopropylacrylamide) prepared by frontal polymerization, J. Mater. Chem. 21 (2011) 8727–8733, https://doi.org/10.1039/C1JM11076D.

[46] A. Das, A. Babu, S. Chakraborty, J.F.R. Van Guyse, R. Hoogenboom, S. Maji, Poly (N-isopropylacrylamide) and its copolymers: a review on recent advances in the areas of sensing and biosensing, Adv. Funct. Mater. 34 (2024) 2402432, https://doi.org/10.1002/adfm.202402432.

[47] J. Hua, P.F. Ng, B. Fei, High-strength hydrogels: Microstructure design, characterization and applications, J. Polym. Sci. B Polym. Phys. 56 (2018) 1325–1335, https://doi.org/10.1002/polb.24725.

[48] G.L. Puleo, F. Zulli, M. Piovanelli, M. Giordano, B. Mazzolai, L. Beccai, L. Andreozzi, Mechanical and rheological behavior of pNIPAAM crosslinked macrohydrogel, React. Funct. Polym. 73 (2013) 1306–1318, https://doi.org/10.1016/j.reactfunctpolym.2013.07.004.

[49] T.R. Matzelle, G. Geuskens, N. Kruse, Elastic properties of Poly(N-isopropylacrylamide) and poly(acrylamide) hydrogels studied by scanning force microscopy, Macromolecules 36 (2003) 2926–2931, https://doi.org/10.1021/ma021719p.

[50] X. Ma, Y. Li, W. Wang, Q. Ji, Y. Xia, Temperature-sensitive poly(N-isopropylacrylamide)/graphene oxide nanocomposite hydrogels by in situ polymerization with improved swelling capability and mechanical behavior, Eur. Polym. J. 49 (2013) 389–396, https://doi.org/10.1016/j.eurpolymj.2012.10.034.

[51] J. Wang, L. Lin, Q. Cheng, L. Jiang, A strong bio-inspired layered PNIPAM-clay nanocomposite hydrogel, Angew. Chem. Int. Ed. 51 (2012) 4676–4680, https://doi.org/10.1002/anie.201200267.

[52] F. Proescher, Oil red O pyridin, a rapid fat stain, Stai. Technol. 2 (1927) 60–61, https://doi.org/10.3109/10520292709115655.

[53] J.J. Nunnari, T. Zand, I. Joris, G. Majno, Quantification of oil red O staining of the aorta in hypercholesterolemic rats, Exp. Mol. Pathol. 51 (1989) 1–8, https://doi.org/10.1016/0014-4800(89)90002-6.

[54] Y. Wang, Y. Fan, P. Zhang, L. Tian, J. Xu, S. Niu, L. Ren, J. Zhao, W. Ming, Dynamically oleophobic epoxy coating with surface enriched in silicone, Prog. Org. Coat. 154 (2021) 106170, https://doi.org/10.1016/j.porgcoat.2021.106170.

[55] Z. Li, B. Wang, X. Qin, Y. Wang, C. Liu, Q. Shao, N. Wang, J. Zhang, Z. Wang, C. Shen, Z. Guo, Superhydrophobic/superoleophilic polycarbonate/carbon nanotubes porous monolith for selective oil adsorption from water, ACS Sustain. Chem. Eng. 6 (2018) 13747–13755, https://doi.org/10.1021/acssuschemeng.8b01637.

[56] Y. Zhu, Y. Du, J. Su, Y. Mo, S. Yu, Z. Wang, Durable superhydrophobic melamine sponge based on polybenzoxazine and Fe_3O_4 for oil/water separation, Sep. Purif. Technol. 275 (2021) 119130, https://doi.org/10.1016/j.seppur.2021.119130.

[57] D. Kuckling, C.D. Vo, H.-J.-P. Adler, A. Völkel, H. Cölfen, Preparation and characterization of photo-cross-linked thermosensitive PNIPAAm nanogels, Macromolecules 39 (2006) 1585, https://doi.org/10.1021/ma052227q.

[58] Q. Zhang, T. Zhang, T. He, L. Chen, Removal of crystal violet by clay/PNIPAm nanocomposite hydrogels with various clay contents, Appl. Clay Sci. 90 (2014) 1–5, https://doi.org/10.1016/j.clay.2014.01.003.

[59] T. Nakamura, M. Ogawa, Adsorption of cationic dyes within spherical particles of poly(N-isopropylacrylamide) hydrogel containing smectite, Appl. Clay Sci. 83–84 (2013) 469–473, https://doi.org/10.1016/j.clay.2013.05.005.

[60] X. Zhou, J. Wang, J. Nie, B. Du, Poly(N-isopropylacrylamide)-based ionic hydrogels: synthesis, swelling properties, interfacial adsorption and release of dyes, Polym. J. 48 (2016) 431–438, https://doi.org/10.1038/pj.2015.123.

[61] J.G. Vijayan, T.N. Prabhu, K. Pal, Poly(N-isopropylacrylamide)-co-poly(sodium acrylate) hydrogel for the adsorption of cationic dyes from aqueous solution, Eur. Phys. J. E 46 (2023) 11, https://doi.org/10.1140/epje/s10189-023-00266-x.

[62] Z. Cui, B.H. Lee, C. Pauken, B.L. Vernon, Degradation, cytotoxicity, and biocompatibility of NIPAAm-based thermosensitive, injectable, and bioresorbable polymer hydrogels, J. Biomed. Mater. Res. A 98A (2011) 159–166, https://doi.org/10.1002/jbm.a.33093.

[63] H. Li, H. Sun, Y. Liu, B. Yuan, J. Hu, Y. Jiang, Q. Li, S. Cao, H. Liu, B. Xiao, P. Shi, X. Yang, S. Wang, Y. Zhao, Toxicology and safety research of poly(N-

isopropylacrylamide)-based thermosensitive nanogels, Environ. Sci.; Nano 10 (2023) 3357–3365, https://doi.org/10.1039/D3EN00206C.
[64] H. Vihola, A. Laukkanen, L. Valtola, H. Tenhu, J. Hirvonen, Cytotoxicity of thermosensitive polymers poly(N-isopropylacrylamide), poly(N-vinylcaprolactam) and amphiphilically modified poly(N-vinylcaprolactam), Biomaterials 26 (2005) 3055–3064, https://doi.org/10.1016/j.biomaterials.2004.09.008.
[65] R. Bilardo, F. Traldi, C.H. Brennan, M. Resmini, The role of crosslinker content of positively charged NIPAM nanogels on the in vivo toxicity in zebrafish, Pharmaceutics 15 (2023) 1900, https://doi.org/10.3390/pharmaceutics15071900.
[66] L. Fu, L. Yang, C. Dai, C. Zhao, L. Ma, Thermal and mechanical properties of acrylated expoxidized-soybean oil-based thermosets, J. Appl. Polym. Sci. 117 (2010) 2220–2225, https://doi.org/10.1002/app.32126.
[67] D. Sibilia, M. Amendolea, R. Sangiovanni, M. Bragaglia, F. Nicoletti, P. Filetici, A. D'Addona, F. Nanni, L. Dassatti, G. Nocca, Biodegradation study of biomaterials composed of acrylated epoxidized soybean oil: an in vitro study, Biomed Res. Int. 2024 (2024) 7100988, https://doi.org/10.1155/bmri/7100988.
[68] A. Zych, J. Tellers, L. Bertolacci, L. Ceseracciu, L. Marini, G. Mancini, A. Athanassiou, Biobased, biodegradable, self-healing boronic ester vitrimers from epoxidized soybean oil acrylate, ACS Appl. Polym. Mater. 3 (2021) 1135–1144, https://doi.org/10.1021/acsapm.0c01335.